



Effects of Al and Ni doping on oxidation and corrosion resistance of electrophoretic deposited YSZ coatings

Li-li WANG, Wei WANG, Ye-li FAN, Xiao-xiao QI, Ji-hua LIU, Zi-ying ZHANG

School of Materials Engineering, Shanghai University of Engineering Science, Shanghai 201620, China

Received 16 March 2016; accepted 1 September 2016

Abstract: Ytria-stabilized zirconia (YSZ)/(Ni,Al) coatings were deposited on Inconel 600 alloy substrate by the electrophoretic deposition combined with vacuum sintering technique. The effects of isothermal oxidation at 1100 °C on the composition of the coatings and the crack healing were investigated, and the corrosion resistance of the coatings in 3.5% NaCl (mass fraction) solution was also studied. The results showed that the cracks on the coating gradually healed up with the increase of the isothermal oxidation time. During isothermal oxidation process, the coating composed of Ni₃Al was transformed to α -Al₂O₃ particulates. The α -Al₂O₃ particulates can seal the defects such as pores and cracks, and meanwhile prevent the oxygen diffusion into the coatings. The polarization curves and EIS results indicated that the coatings oxidized for 40 h had a more positive corrosion potential, higher breakdown potential, higher impedance module at low frequency and much lower corrosion current density compared with YSZ coated and uncoated Inconel 600 alloys.

Key words: electrophoretic deposition; corrosion; composite coating; superalloy

1 Introduction

Inconel 600 alloys have been widely applied as the structure materials in the pressurized water reactor nuclear power plant such as the steam generator tube materials due to their high formability and corrosion resistance [1]. However, they show susceptibility against the inter-granular stress corrosion cracking [2–4]. The pitting corrosion of the stream generating tubes emerged as a main cause of the tube failure since the 1970s [5]. The reasons for these damages were sludge, acid chloride, oxidizing conditions and operating temperature. Efforts have been made to improve the corrosion resistance by surface modification, including ion implantation [6,7] and laser surface melting [8]. However, such physical methods can produce open pores and pinholes on the treated surface due to the high energy ion collision. Surface defects cause a local corrosion of Inconel 600 alloy under the attack of aqueous and/or gaseous corrosive environments.

Recently, electrophoretic deposition (EPD) has been recommended due to its simplicity, controlled chemical composition and microstructure [9,10]. However, the

appearance of cracks on coating surfaces as a result of shrinkage during sintering severely limits its widespread uses [11,12]. Reaction bonding is a forming technique developed to produce near net shape ceramics and overcome problems caused by shrinkage during sintering.

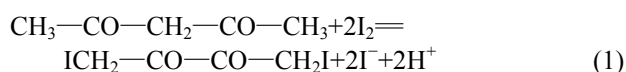
Ytria-stabilized zirconia (YSZ) has been employed as a protective coating on various metals and their alloys owing to its high chemical stability and excellent corrosion resistance [13–15]. In addition, Al₂O₃ is also used in ceramic compositions. α -Al₂O₃ can surround the YSZ crystals as a hard matrix and prevent its phase transformation by the creation of compressive stresses. Our research groups had reported that YSZ/(Ni,Al) composite coating fabricated by EPD exhibited self-healing due to the formation of α -Al₂O₃ by oxidation [16]. It seems that a particulate or layered composite of YSZ with α -Al₂O₃ protects the substrate from oxidation and corrosion. There has been few published information concerning corrosion resistance of self-healing YSZ composite coatings containing Al and Ni particles. The aim of this work is to study the effects of vacuum sintering, Al/Ni doping and oxidation treatment on corrosion resistance of YSZ composite coatings.

In this work, YSZ composite coatings containing Al and Ni particles (YSZ/(Ni,Al)) were deposited on Inconel 600 alloy by EPD combined with vacuum sintering technique, and their electrochemical corrosion properties were investigated.

2 Experimental

2.1 Materials

The Inconel 600 alloys were used as the substrate. Specimens in the form of plates with dimensions of 20 mm × 20 mm × 3 mm were cut and polished to a mirror finish with 1 μm Al₂O₃ powder, then degreased by detergent and further ultrasonically cleaned with acetone. 92% YSZ powder and 4% Al and 4% Ni (mass fraction) powders were mixed with acetylacetone. The suspension was stirred with a magnetic stirrer for 10 min. The concentration of suspension was 40 g/L. Small amount of iodine (0.4 g/L) was added to the solution and stirred with ultrasonic for 3 h by a high intensity ultrasonic probe. It was reported that protons were formed by a reaction between acetylacetone and iodine. The reaction of iodine with acetylacetone can be represented by Eq. (1).



The adsorption of the formed protons onto the suspended particles will make them positively charged. The application of a direct current electric field causes the positively charged particles to move towards and deposit on the cathode. In addition, polyvinyl alcohol was used as a dispersant to help disperse powders and reduce agglomeration.

2.2 Electrophoretic deposition of composite coatings

Graphite electrode and the substrate were used as the anode and cathode, respectively. The electrodes were placed parallel and immersed in the suspension. The distance between electrodes was kept at 30 mm. The EPD process was performed using a constant voltage of 120 V at room temperature. The green coatings were dried at room temperature for 24 h. The sintering of EPD-coated samples was performed at 1100 °C for 2 h under vacuum (6.67×10^{-3} Pa) and then furnace was cooled to room temperature.

2.3 Characterization

2.3.1 Surface morphology and microstructure analysis

The surface morphology and cross-section of the coatings were observed by scanning electron microscopy (SEM, S-3400N) and field-emission-gun environment scanning electron microscopy (FESEM, JSM-6700F). X-ray diffraction (XRD, DLMAX-2200) was

employed to study the phase composition.

2.3.2 Electrochemical tests

Anodic polarization curves were carried out using a potentiostat system (VersaSTAT 3F). The 3.5% NaCl solution was kept at room temperature. A saturated calomel electrode (SCE) was used as the reference electrode and two parallel platinum electrodes served as the counter electrode for current measurement. To avoid crevice corrosion, the protective tape was used to mask samples, allowing 1 cm² of the surface to be in contact with the solution. Anodic polarization curves were recorded between -500 and +700 mV over the corrosion potential at a scan rate of 0.2 mV/s. Electrochemical impedance spectroscopy (EIS) measurements were performed in 3.5% NaCl solution at room temperature. The frequency was varied from 10⁵ to 0.1 Hz with an applied AC voltage of ±10 mV with respect to the open circuit potential. The obtained impedance data were analyzed by the software (versaStudio). The corrosion tests were repeated at least five times for reliability and reproducibility.

3 Results and discussion

3.1 Characteristics of coatings

YSZ/(Ni,Al) composite coatings were carried out to promote chemical reaction between aluminum and nickel which will enhance sintering at a relatively low temperature. Figure 1 shows the XRD patterns of the coatings after being isothermally oxidized at 1100 °C for different time. It can be seen that the phase constitutions varied with oxidation time. Figure 1(a) shows the XRD pattern of as-vacuum sintered YSZ/(Ni,Al) composite coatings. It can be seen that the composite coatings mainly consist of tetragonal ZrO₂ and AlNi₃. An AlNi₃ phase in the composite coatings is usually resistant to

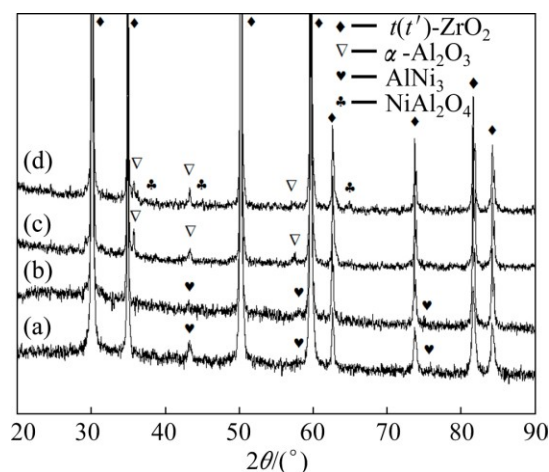


Fig. 1 XRD patterns of YSZ/(Ni,Al) composite coatings after isothermal oxidation at 1100 °C in air for different time: (a) As-vacuum sintered; (b) 20 h; (c) 40 h; (d) 60 h

corrosion in aqueous acidic corrosion environments [17]. For the YSZ/(Ni,Al) composite coatings after being isothermally oxidized for 20 h, as shown in Fig. 1(b), the products still consist of tetragonal ZrO_2 and $AlNi_3$. Figure 1(c) shows the presence of tetragonal ZrO_2 , $\alpha-Al_2O_3$ on the coated samples after being isothermally oxidized for 40 h. In contrast, complex oxide products including tetragonal ZrO_2 , $\alpha-Al_2O_3$ and $NiAl_2O_4$ were detected after being isothermally oxidized for 60 h, as shown in Fig. 1(d).

For YSZ/(Ni,Al) coated sample, oxidation at 1100 °C causes decomposition of $AlNi_3$ phase. The relevant oxidation reactions are as follows:



Figure 2 shows the cross-sectional morphologies of

the YSZ/(Ni,Al) coated samples after being isothermally oxidized at 1100 °C in air for different time. It can be observed that all coated samples were around 45 μm in thickness and had good adhesion to the substrate. No visible impenetrable crack existed in the coated samples. Moreover, somewhat larger pores (marked with arrows in Fig. 2(a)) were observed in the as-vacuum sintered composite coatings. In contrast, after being isothermally oxidized at 1100 °C for 20 h, the composite coating contained smaller submicron pores (marked with arrows in Fig. 2(b)). After isothermal oxidation at 1100 °C in air for 40 h, the coated samples exhibited a relatively dense, pore-free microstructure, as shown in Fig. 2(c). However, after being isothermally oxidized at 1100 °C in air for 60 h, some submicron pores (marked with arrows in Fig. 2(d)) were observed again in the coated sample.

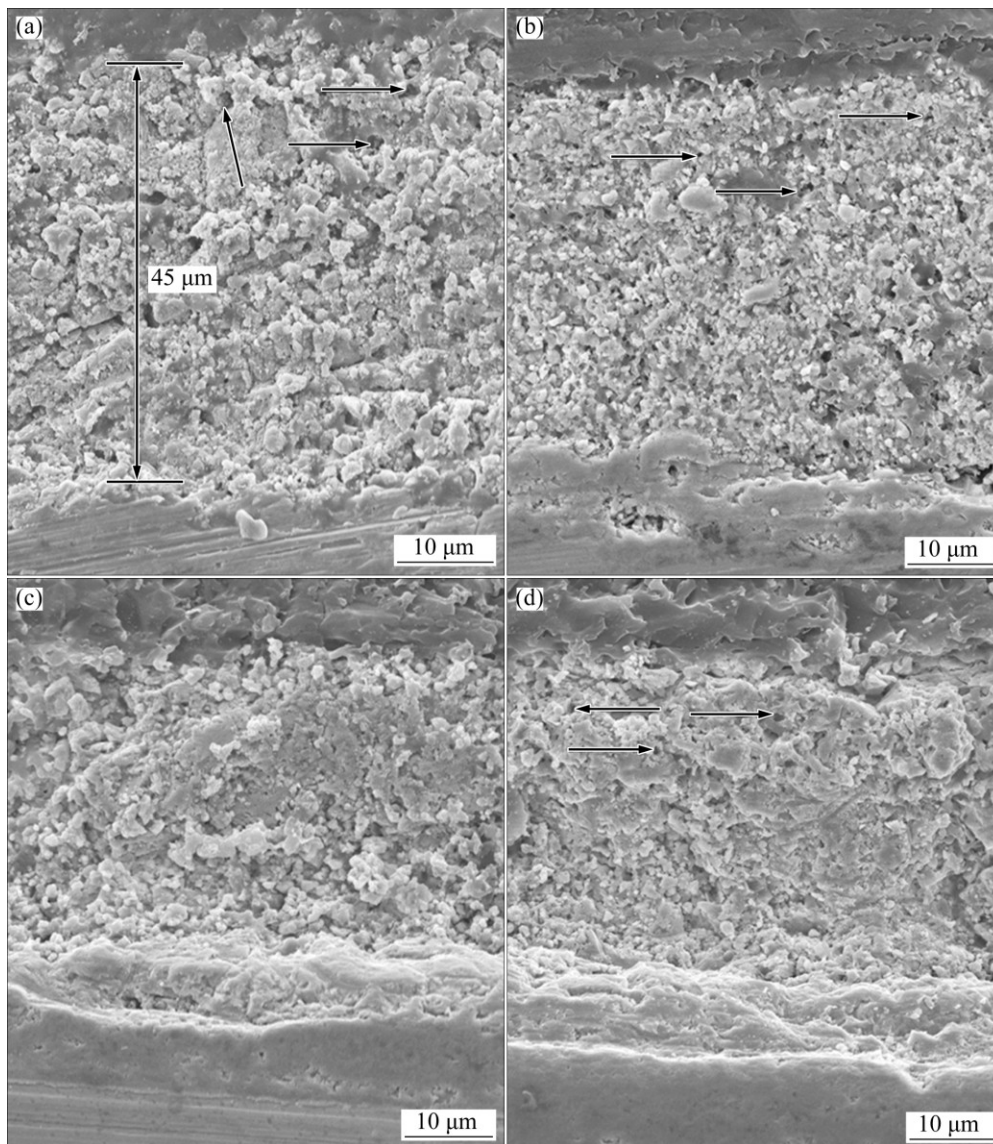


Fig. 2 Cross-sectional micrographs of YSZ/(Ni,Al) composite coatings after isothermal oxidation at 1100 °C in air for different time: (a) As-vacuum sintered; (b) 20 h; (c) 40 h; (d) 60 h

It should be noted that the most important difference in microstructure between the as-vacuum sintered and oxidized samples was the size of porosities. In the composite coating oxidized at 1100 °C for 20 h, the porosities had the same size and were distributed uniformly. But in the as-vacuum sintered sample, the porosities had different sizes. The formation of larger pores may be due to the phase transformation (the formation of AlNi_3 phase) which resulted in stress mismatches in the composite coatings during vacuum sintering. Taking into account the formation of $\alpha\text{-Al}_2\text{O}_3$ particulates (Fig. 1(c)), it is believed that the $\alpha\text{-Al}_2\text{O}_3$ particulates can seal the defects such as pores in time and meanwhile prevent the oxygen diffusion into the coatings (Fig. 2(c)). With the increase of oxidation time (oxidation for 60 h), detrimental spinel-type NiAl_2O_4 oxide was formed. The NiAl_2O_4 oxide continued growing, and submicron pores were formed between the NiAl_2O_4 oxide and coating. FEGE-SEM was utilized to investigate the surface oxide morphology of YSZ/(Ni,Al) composite coatings oxidized for 60 h. Figure 3 proved that the oxide scale was composed of $\alpha\text{-Al}_2\text{O}_3$ and spinel-type NiAl_2O_4 oxide, which was in agreement with the XRD results shown in Fig. 1(d). For the sample oxidized for 60 h, a crater (not shown here) with porous structure was observed on the surface. It is speculated that the formation of a crater should be related to spinel-type NiAl_2O_4 oxide. In corrosive environment, this type of defect is expected to form a penetrated pathway and leads to the formation of a galvanic cell. Meanwhile, pitting corrosion starts due to the potential differences between NiAl_2O_4 oxide and YSZ coating.

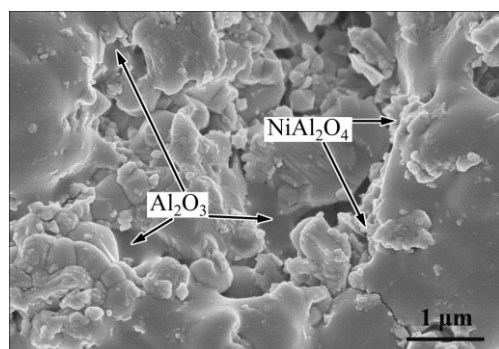


Fig. 3 FEGE-SEM morphology of YSZ/(Ni,Al) composite coatings after isothermal oxidation at 1100 °C in air for 60 h

3.2 Corrosion properties of Inconel 600 substrate and YSZ coated samples

To study the effect of oxidation time on the corrosion resistance of YSZ/(Ni,Al) composite coatings, polarization measurements were performed in 3.5% NaCl solution to evaluate corrosion resistance of YSZ/(Ni,Al) composite coatings. The Inconel 600

substrate and as-vacuum sintered YSZ coated samples had also been included for comparison. Figure 4 presents the potentiodynamic polarization curves of as-vacuum sintered YSZ coated samples and Inconel 600 substrate. From both experimental curves, corrosion potential (ϕ_{corr}) and corrosion current density (J_{corr}) were determined using the Echem analyst software. The determined potentiodynamic parameters are summarized in Table 1. For the Inconel 600 substrate, ϕ_{corr} and J_{corr} were determined to be -713 mV (vs SCE) and 3.43×10^{-5} A/cm², respectively. Compared with the uncoated substrate, the as-vacuum sintered YSZ coated samples had more positive corrosion potential (-268 mV (vs SCE)), much lower corrosion current density (2.09×10^{-5} A/cm²), which can be attributed to the formation of a thick YSZ coating that leads to delaying the contact between the corrosive species and Inconel 600 substrate. However, the potentiodynamic polarization curve for the as-vacuum sintered YSZ coated samples in Fig. 4 does not show a passive range and the breakdown of the passive film takes place at the open circuit potential. This indicates that the deposited YSZ composite coatings cannot protect the substrate, providing a significant barrier against localized attack.

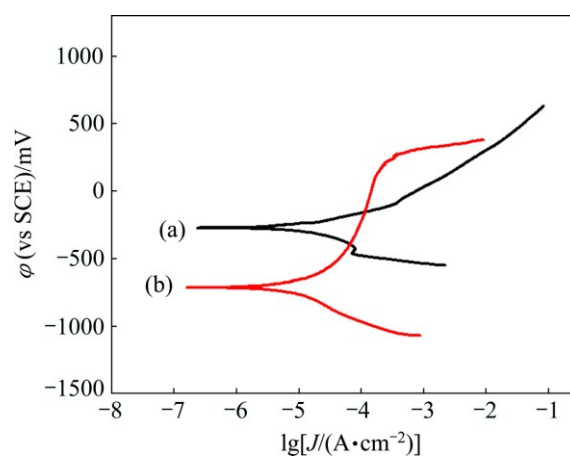


Fig. 4 Potentiodynamic polarization curves in 3.5% NaCl solution for as-vacuum sintered YSZ coated samples (a) and uncoated Inconel 600 alloy (b)

Table 1 Potentiodynamic polarization results for YSZ coating and substrate

Sample	$\phi_{\text{corr}}/\text{mV}$	$J_{\text{corr}}/(\text{A}\cdot\text{cm}^{-2})$
As-vacuum sintered YSZ coating	-268	2.09×10^{-5}
Substrate	-713	3.43×10^{-5}

3.3 Corrosion properties of oxidizing YSZ/(Ni,Al) coated samples

Figure 5 shows the potentiodynamic polarization curves for YSZ/(Ni,Al) coated samples oxidized at

1100 °C in air for different time. The determined potentiodynamic parameters are summarized in Table 2.

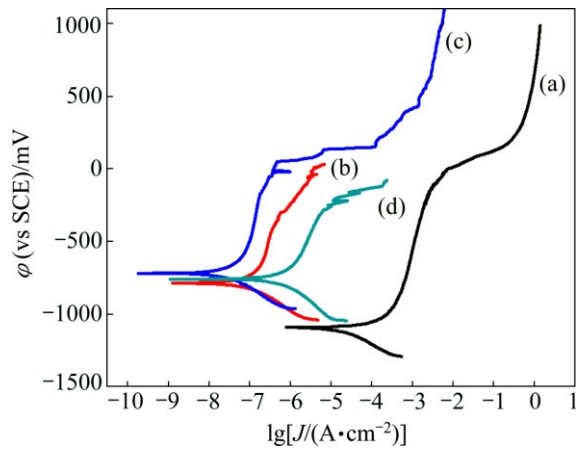


Fig. 5 Potentiodynamic polarization curves in 3.5% NaCl solution for oxidizing YSZ/(Ni,Al) coated samples: (a) As-vacuum sintered; (b) Oxidized for 20 h; (c) Oxidized for 40 h; (d) Oxidized for 60 h

Table 2 Potentiodynamic polarization results for oxidizing YSZ/(Ni,Al) coated samples

Sample	$\phi_{\text{corr}}/\text{mV}$	$J_{\text{corr}}/(\text{A}\cdot\text{cm}^{-2})$	$\phi_{\text{pass}}/\text{mV}$
As-vacuum sintered YSZ/(Ni,Al) coating	-589	2.96×10^{-5}	381
Coating oxidized for 20 h	-285	2.85×10^{-7}	197
Coating oxidized for 40 h	-221	5.01×10^{-8}	532
Coating oxidized for 60 h	-257	1.29×10^{-6}	283

Although the YSZ/(Ni,Al) composite coatings exhibited consolidation by oxidation, the formation of droplets (metal-rich particles) and/or inclusions (detrimental spinel-type mixed oxides) in high-temperature oxidation environments tends to lower the oxidation/corrosion resistance [18]. At the beginning, the composite coatings could be consolidated spontaneously, and corrosion resistance was improved quickly. With the increase of the oxidation time, the droplets and/or inclusions (detrimental spinel-type oxides) were formed. The main reason for the corrosion behavior of the YSZ/(Ni,Al) composite coatings is that once a droplet is formed, the defects continue growing throughout the coatings and an interface is formed between the defect and coating. Therefore, penetrated pathways are formed between the defect and corrosive medium, which finally lead to the formation of a galvanic corrosion cell. Moreover, the growth defects cause a local corrosion of the coatings and the substrate under the attack of the corrosive environments. It is obvious that the YSZ/(Ni,Al) composite coating oxidized for 40 h exhibits the best corrosion resistance. The highest ϕ_{corr} and lowest J_{corr} were determined to be -221 mV (vs SCE)

and 5.01×10^{-8} A/cm², respectively, as shown in Table 2. Also, the highest breakdown potential was determined to be 532 mV (vs SCE). However, after being isothermally oxidized at 1100 °C in air for less than 40 h or more, the composite coating could not obtain excellent corrosion resistance. Even then, the corrosion current density of all coatings, which go through an oxidation process, is lower than that without oxidation, and ϕ_{corr} is shifted in noble direction and J_{corr} is decreased by one or two orders of magnitude compared with those of uncoated Inconel 600 alloys (Fig. 4).

The corrosion properties of YSZ/(Ni,Al) composite coatings were also evaluated using EIS. Figure 6 shows Bode plot of the impedance modulus of oxidized YSZ/(Ni,Al) coated samples. It can be seen that the composite coating after being isothermally oxidized for 40 h exhibits the highest impedance module ($\sim 10^7$ Ω·cm²) at low frequency. This indicates that oxidation for 40 h provides good barrier properties. As reported by SHABANI-NOOSHABADI et al [19], the coating porosity plays a significant role in anticorrosive properties. These pores provide an electrolytic track to the alloy surface and results in localized corrosion sites which ultimately lead to the increase in corrosion rate. It is reported that the coating porosity is related not only to the alumina mixing ratio but also to the coating thickness [20]. Nevertheless, in the present study, all coated samples were of almost the same thickness, accordingly, the increase in corrosion resistance of YSZ/(Ni,Al) coated samples oxidized for 40 h may be attributed to the reduction of pores through the formation of more stable and inert α -Al₂O₃ oxide, thus preventing the corrosion process at coating/substrate interface. A protective oxide on the oxidized samples is also visible at high frequency as compared with as-vacuum sintered sample, as shown in Fig. 6(c).

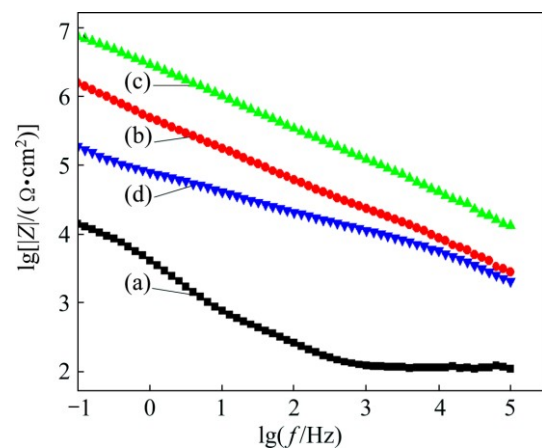


Fig. 6 Bode plot of impedance modulus of oxidized YSZ/(Ni,Al) coated samples after immersion in 3.5% NaCl solution for 2 h: (a) As-vacuum sintered; (b) Oxidized for 20 h; (c) Oxidized for 40 h; (d) Oxidized for 60 h

Based on electrochemical corrosion test results and the morphology of the coatings, it can be concluded that corrosion protection of the Inconel 600 alloys is significantly enhanced by YSZ/(Ni,Al) composite coating oxidized for 40 h at 1100 °C.

4 Conclusions

1) A new approach was proposed to improve the corrosion resistance of Inconel 600 alloy by EPD combined vacuum sintering technique, followed by isothermal oxidation at 1100 °C in air. Evolution of the oxidation morphology indicated that dense α -Al₂O₃ particulates formed in the defects.

2) The potentiodynamic and EIS tests revealed that corrosion protection of the Inconel 600 alloys was significantly enhanced by oxidizing YSZ/(Ni,Al) composite coating. The YSZ/(Ni,Al) composite coating oxidized for 40 h exhibited a relatively high corrosion resistance. The corrosion potential, breakdown potential and corrosion current density were determined to be -221 mV (vs SCE), 532 mV (vs SCE) and 5.01×10^{-8} A/cm², respectively.

References

- [1] HU H X, ZHENG Y G, QIN C P. Comparison of Inconel 625 and Inconel 600 in resistance to cavitation erosion and jet impingement erosion [J]. Nuclear Engineering and Design, 2010, 240(10): 2721–2730.
- [2] ASHOUR E A. Crack growth rates of Inconel 600 in aqueous solutions at elevated temperature [J]. Journal of Materials Science, 2001, 36(3): 685–692.
- [3] KIM J D, MOON J H. C-ring stress corrosion test for Inconel 600 and Inconel 690 sleeve joint welded by Nd: YAG laser [J]. Corrosion Science, 2004, 46(4): 807–818.
- [4] PENG Q, HOU J, SAKAGUCHI K, TAKEDA Y, SHOJI T. Effect of dissolved hydrogen on corrosion of Inconel alloy 600 in high temperature hydrogenate water [J]. Electrochimica Acta, 2011, 56(24): 8375–8386.
- [5] IN C B, KIM Y I, KIM W W, KIM J S, CHUN S S, LEE W J. Pitting resistance and mechanism of TiN-coated Inconel 600 in 100 °C NaCl solution [J]. Journal of Nuclear Materials, 1995, 224(1): 71–78.
- [6] SISTA V, KAHVECIOGLU O, KARTAL G, ZENG Q Z, KIM J H, ERYILMAZ Q L, ERDEMIR A. Evaluation of electrochemical boriding of Inconel 600 [J]. Surface & Coatings Technology, 2013, 215: 452–459.
- [7] DEEN K M, AFZAL N, AHMAD R, NIAZI Z, AYUB R, FAROOQ A, KHAN I H, KHALEEQ-UR-RAHMAN M. Intergranular pitting tendency of yttrium implanted Inconel 600 in acidic chloride media [J]. Surface & Coatings Technology, 2012, 212(6): 61–66.
- [8] BAO G, SHINOZAKI K, INKYO M, MIYOSHI T, YAMAMOTO M, MAHARA Y, WATANABE H. Modeling of precipitation and Cr depletion profiles of Inconel 600 during heat treatments and LSM procedure [J]. Journal of Alloys & Compounds, 2006, 419(1–2): 118–125.
- [9] LUO Qing-wei, LI Ying-nan, LI Feng-hua, FAN Zhan-guo. Preparation of YBa₂Cu₃O_{7- δ} superconducting thick film on Ni–W tapes via electrophoretic deposition [J]. Transactions of Nonferrous Metals Society of China, 2014, 24(1): 120–125.
- [10] DOU Yuan-yun, LUO Min, LIANG Sen, ZHANG Xue-ling, DING Xiao-yi, LIANG Bin. Flexible free-standing graphene-like film electrode for supercapacitors by electrophoretic deposition and electrochemical reduction [J]. Transactions of Nonferrous Metals Society of China, 2014, 24(5): 1425–1433.
- [11] WANG Z, XIAO P, SHEMILT J. Fabrication of composite coatings using a combination of electrochemical methods and reaction bonding process [J]. Journal of the European Ceramic Society, 2000, 20(10): 1469–1473.
- [12] JI Chang-zheng, LAN Wei-hua, XIAO Ping. Fabrication of yttria-stabilized zirconia coatings using electrophoretic deposition: Packing mechanism during deposition [J]. Journal of the American Ceramic Society, 2008, 91(4): 1102–1109.
- [13] RYU H S, LIM T S, RYU J, HONG S H. Corrosion protection performance of YSZ coating on AA7075 aluminum alloy prepared by aerosol deposition [J]. Journal of the Electrochemical Society, 2013, 160(1): C42–C47.
- [14] TIWARI S K, ADHIKARY J, SINGH T B, SINGH R. Preparation and characterization of sol–gel derived yttria doped zirconia coating on AISI 316L [J]. Thin Solid Films, 2009, 517(16): 4502–4508.
- [15] AMAYA C, APERADOR W, CAICEDO J C, ESPINOZA-BELTRAN F J, MUNOZ-SALDANA J, ZAMBRANO G, PRIETO P. Corrosion study of alumina/yttria-stabilized zirconia (Al₂O₃/YSZ) nanostructured thermal barrier coatings (TBC) exposed to high temperature treatment [J]. Corrosion Science, 2009, 51(12): 2994–2999.
- [16] LI Cun-ling, WANG Wei, TAN Shi-lei, SONG Shan-guang. Bond strength and oxidation resistance of YSZ/(Ni,Al) composite [J]. Surface Engineering, 2014, 30(9): 619–623.
- [17] KIM H J, WALTER M E. Characterization of the degraded microstructures of a platinum aluminide coating [J]. Materials Science and Engineering A, 2003, 360(1–2): 7–17.
- [18] LEWIS D B, CREASEY S J, WUSTEFELD C, EHIASARIAN P, HOVEPIAN P E. The role of the growth defects on the corrosion resistance of CrN/NbN superlattice coatings deposited at low temperatures [J]. Thin Solid Films, 2006, 503(1–2): 143–148.
- [19] SHABANI-NOOSHABADI M, GHOREISHI S M, BEHPOUR M. Electropolymerized polyaniline coatings on aluminum alloy 3004 and their corrosion protection performance [J]. Electrochimica Acta, 2009, 54(27): 6989–6995.
- [20] ZHANG J L, KOBAYASHI A. Corrosion resistance of the Al₂O₃+ZrO₂ thermal barrier coatings on stainless steel substrates [J]. Vacuum, 2008, 83(1): 92–97.

掺杂 Ni、Al 对 YSZ 电泳沉积涂层 抗氧化和腐蚀性能的影响

王莉莉, 王伟, 范焯力, 戚哮啸, 刘继华, 张子英

上海工程技术大学 材料工程学院, 上海 201620

摘 要: 使用电泳沉积和真空烧结技术在 Inconel 600 合金基体上沉积 YSZ/(Ni,Al)涂层, 研究在 1100 °C 等温氧化过程中涂层的组成、表面裂纹的自愈合性以及涂层在 3.5%氯化钠(质量分数)溶液中的电化学腐蚀性能。结果表明, 随着氧化时间的延长, 涂层表面上的裂纹逐渐愈合。在恒温氧化过程中涂层中的 Ni_3Al 转化成 $\alpha\text{-Al}_2\text{O}_3$ 微粒, $\alpha\text{-Al}_2\text{O}_3$ 微粒能够对涂层表面的裂纹和气孔等缺陷进行密封, 从而阻止氧气扩散到涂层内部。极化曲线和阻抗的测定结果表明, 涂层在恒温氧化 40 h 时有较高的自腐蚀和击穿电位, 在低频下有更高的阻抗模值, 与基体和纯 YSZ 涂层相比有更低的自腐蚀电流密度。

关键词: 电泳沉积; 腐蚀; 复合涂层; 高温合金

(Edited by Wei-ping CHEN)